

Enhancement of DNA-mediated Energy Transfer from Ethidium to *meso*-Tetrakis(*N*-methylpyridinium-4-yl)porphyrin by Ca^{2+} Ion

Jong-Moon Kim, Borami Park, Young Rhan Kim, Lindan Gong, Myung Duk Jang,[†] and Seog K. Kim^{*}

Department of Chemistry, Yeungnam University, Gyeong-buk 712-749, Korea. *E-mail: seogkim@yu.ac.kr

[†]Department of Gas-Energy Engineering, Kundong University, Gyeongbuk 760-833, Korea

Received November 22, 2011, Accepted December 29, 2011

The fluorescence intensity of DNA-intercalated ethidium with [ethidium]/[DNA base] being 0.005 was quenched upon the binding of another intercalating ligand, *meso*-tetrakis(*N*-methylpyridinium-4-yl)porphyrin (TMPyP). Addition of Ca^{2+} enhanced the quenching efficiency. The range of separations between donor and acceptor molecules, within which total quenching occurs, was calculated using a one-dimensional resonance energy transfer mechanism to be 9.5 base-pairs or 32.3 Å in the absence of Ca^{2+} ions. The distance increased to 18.7 base-pairs or about 63.6 Å in the presence 100 μM Ca^{2+} . Considering that (1) Ca^{2+} had little effect on the binding modes of ethidium and TMPyP, which was investigated by reduced linear dichroism and (2) spectral overlap between the emission spectrum of ethidium and the absorption spectrum of TMPyP was maintained in the presence of Ca^{2+} , contributions from orientation factor and spectral overlap to Ca^{2+} -induced enhancement in DNA mediated energy transfer was limited. Although there is no direct evidence, electron transfer along the DNA stem may accompany the observed fluorescence quenching. In this respect, DNA bound Ca^{2+} act as a partially conducting medium.

Key Words : Energy transfer, Porphyrin, Ethidium, DNA, Ca^{2+}

Introduction

DNA has long been investigated as a medium of charge¹⁻⁶ and energy transfer⁷⁻¹⁵ through its bases' stacked π -orbitals. Fluorescence resonance energy transfer (RET) has been employed to investigate the helical geometry of double-stranded DNA.¹⁶ It has also been used to measure molecular distances in DNA molecules.¹⁷ Its applications range from investigating the conformational changes of nucleic acids, studying their dynamics within biological processes¹⁸⁻²⁰ and to nanotechnology.²¹⁻²³ These photochemical processes generally involve non-radiative transfer of electronic excitation from an excited donor molecule to a ground state acceptor molecule on time scales of femtoseconds to milliseconds over distances ranging from a few Å to approximately 100 Å. Förster type resonance energy transfer occurs for allowed singlet-singlet transitions if there is significant overlap between the donor molecule's emission and an acceptor molecule's absorption spectra. The critical transfer radii of such transition range from 10 to 100 Å.^{24,25} For example, the excitation energy of ethidium can transfer to *meso*-tetrakis(*N*-methylpyridinium-4-yl)porphyrin (TMPyP) along a DNA stem when both molecules are simultaneously intercalated between the DNA base-pairs.²⁶ RET between other acceptors and donors which were physically complexed with DNA has been also reported.⁹⁻¹⁵ In this work, we report the presence of Ca^{2+} enhance the efficiency of DNA mediated energy transfer. Ethidium and TMPyP were chosen as the donor and acceptor molecules because their intercalative binding modes have been well-established.

Materials and Methods

Materials. Calf thymus DNA was from Worthington (Lakewood, NJ), and was dissolved in 5 mM cacodylate buffer containing 100 mM NaCl and 1 mM EDTA at pH 7.0 by exhaustive shaking at 4 °C. It was then dialyzed several times at 4 °C in 5 mM cacodylate buffer containing 5 mM NaCl at pH 7.0. The latter buffer was used throughout this work. TMPyP was purchased from Midcentury (Chicago, IL). Other chemicals were from Sigma and used without further purification. The concentrations of DNA, ethidium, and TMPyP were determined spectrophotometrically using the extinction coefficients: $\epsilon_{260\text{nm}} = 6700 \text{ cm}^{-1}\text{M}^{-1}$, $\epsilon_{480\text{nm}} = 5800 \text{ cm}^{-1}\text{M}^{-1}$, $\epsilon_{424\text{nm}} = 2.26 \times 10^5 \text{ cm}^{-1}\text{M}^{-1}$, respectively.

Measurements. Absorption spectra were recorded on a Cary 100 Bio UV-vis spectrophotometer. Linear dichroism (LD) spectra were measured using a Jasco 715 spectropolarimeter equipped with a flow-orienting Couvette cell device with inner-rotating cylinder as it was described elsewhere.^{27,28} LD spectra were averaged over several scans when necessary. The measured LD was divided by the isotropic absorption spectrum to give a reduced LD (LD^r), which is related to the angle, α , specifying the orientation of the transition moment of the molecule with respect to the local helix axis of the DNA.

$$LD^r = 1.5S(3\cos^2\alpha - 1) \quad (1)$$

The orientation factor, S , reflects the degree of DNA orientation in the flow, which depends on its contour length and flexibility, and the viscosity and the temperature of the medium.

Steady state fluorescence spectra were recorded on a Jasco FP-777 spectrofluorimeter. During titration, small aliquots of the titrant, TMPyP, were added to the DNA-ethidium solution and volume corrections were made. The emission intensities of DNA bound ethidium were monitored through excitation and emission at 535 nm and 600 nm, respectively. Typical emission spectra of DNA bound TMPyP appeared at 652 nm. All measurements were performed at an ambient temperature.

Results

RET involves the non-radiative transfer of electronically excited energy from excited donor to acceptor molecules. Therefore, the donor's emission intensity decreases with increasing concentration of acceptor. Increased emission intensity from the acceptor is also sometimes observed. Figure 1(a) shows the emission spectrum of ethidium intercalated between DNA base-pairs with increasing concentrations of TMPyP. The emission is generally centered at 592 nm and tails up to 730 nm. Increasing TMPyP concentration resulted in gradual decrease in the emission intensity of

ethidium, and led to a small increase in emission intensity at 652 nm which corresponds to the emission of DNA bound TMPyP. The presence of 2.5 μM TMPyP quenched the ethidium's emission intensity by about 44%. The presence of Ca^{2+} ions enhanced the decrease in the emission intensity of ethidium: the magnitude of ethidium's emission at its maximum (592 nm) decreased to 62% in the presence of 2.5 μM TMPyP while increase in the intensity at 652 nm was more pronounced in the presence of Ca^{2+} (Figure 1(b)).

The ratio of ethidium's emission intensity in the absence (F_0) to presence (F) of TMPyP was plotted with respect to TMPyP concentration ($[Q]$) according to equation (2) (Stern-Volmer plot, Figure 2(a)), with K_{SV} being the Stern-Volmer quenching constant.

$$\frac{F_0}{F} = 1 + K_{SV}[Q] \quad (2)$$

Upward bending curves were apparent at all tested Ca^{2+} concentrations; increasing Ca^{2+} concentration increased the

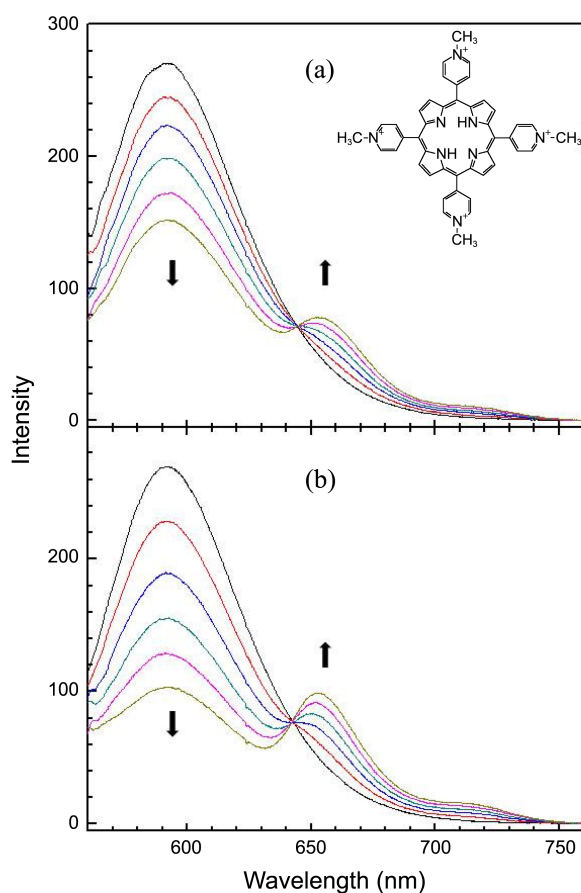


Figure 1. Fluorescence emission spectrum of ethidium intercalated in DNA at various TMPyP concentrations in the absence (panel a) and presence (panel b) of 100 μM Ca^{2+} . $[\text{DNA}] = 100 \mu\text{M}$ and $[\text{ethidium}] = 0.5 \mu\text{M}$. The concentration of TMPyP was 0.0, 0.5, 1.0, 1.5, 2.0, and 2.5 μM in the direction of the arrow. Excitation at 527 nm and slit widths were 10 nm for both excitation and emission. The chemical structure of TMPyP is shown in panel (a).

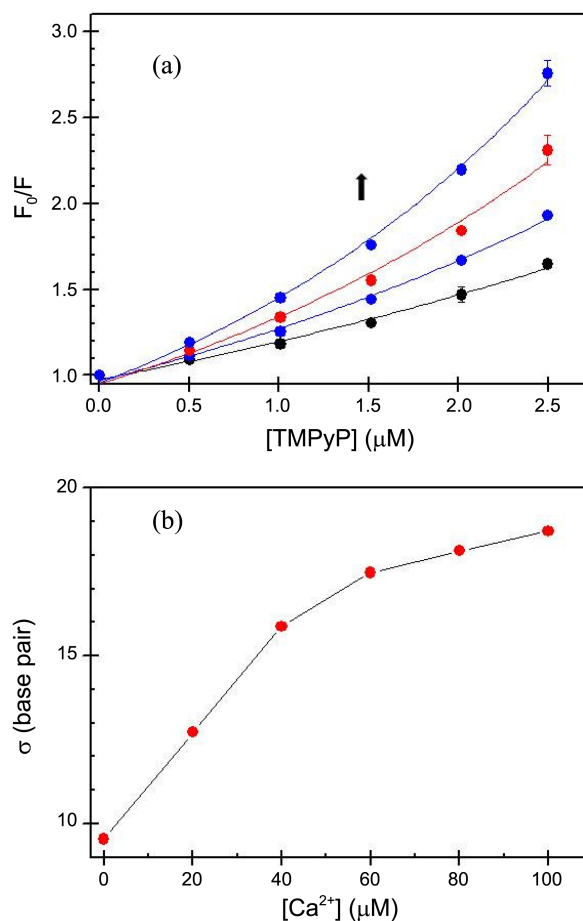


Figure 2. (a) Stern-Volmer plots of the fluorescence quenching of DNA-intercalated ethidium by TMPyP various concentrations of Ca^{2+} . $[\text{Ca}^{2+}]$ increased = 0, 20, 40, 100 μM in the direction of arrow. Representative error bars denoting standard deviations from five measurements are shown. Excitation and emission were 527 nm and 592 nm, respectively. Slit widths were 10 nm for both excitation and emission. Solid curves represent best fits from equation (3). (b) Distance in base-pairs within which ethidium fluorescence was fully quenched occurred with respect to Ca^{2+} concentration. $[\text{DNA}] = 100 \mu\text{M}$ and $[\text{ethidium}] = 0.5 \mu\text{M}$.

quenching efficiency. The observed upward bending curves indicate that quenching was not a simple static or dynamic process. Since the emission spectrum of ethidium and absorption spectrum of TMPyP overlapped (see below), the observed fluorescence quenching involves, at least in part, RET mechanism. In DNA bound acceptor and donor case, one-dimensional RET model proposed by Pasternak *et al.*,²⁴ may be applicable according to equation (3). The best fitted curves from this analysis are also shown in Figure 2 as solid lines.

$$\frac{F_0}{F} = \exp\left\{\frac{2\sigma[Q]}{[DNA]-2[E^+]}\right\} \quad (3)$$

where $[Q]$ is the concentration of TMPyP quencher and $[E^+]$ is the concentration of ethidium. The symbol σ denotes the minimum number of base-pairs between ethidium and TMPyP required to permit the energy transfer between them. Eq. (3) originated from the sphere of action quenching mechanism, which involves defining a critical distance within which the excited energy of the fluorophore is totally deactivated by the quencher.²⁴ Calculated σ values with respect to Ca^{2+} concentration are shown in Figure 2(b). In the absence of Ca^{2+} , the critical distance was 9.5 base-pairs or 32.3 Å, slightly larger than the 25–30 Å reported by Pasternak *et al.*²⁴ The difference may have been due to the differences in the experimental conditions, such as the nature and concentration of the buffer. The distance increased almost linearly with increasing Ca^{2+} concentration up to 40 mM, above which the slope flattened. In 100 mM Ca^{2+} , the critical distance reached 18.7 base-pairs or about 63.6 Å: energy transfer could occur at a distance about twice that observed in the absence of Ca^{2+} .

When the emission energy level of a fluorophore overlaps the absorption energy level of an acceptor, its excited energy can be directly transferred to the acceptor. The overlapping emission energy levels of DNA-intercalated ethidium and absorption energy levels of TMPyP are shown in Figure 3(a). The efficiency of this type of energy transfer is dependent on the spectral overlap between the emission and the absorption spectra ($J(\lambda)$), the relative orientation of both molecules' transition dipoles (κ), the quantum yield of the donor molecule in the absence of the acceptor (Q_D), and the refractive index of the medium (n).²⁵

$$R_0 = (J(\lambda)\kappa^2 Q_D n^{-4})^{1/6} \times 8.79 \times 10^{-25} \text{ in cm} \quad (4)$$

where $J(\lambda) = \int_0^\infty F_D(\lambda)\varepsilon_A(\lambda)\lambda^4 d\lambda$.

In this equation, $F_D(\lambda)$ is the normalized fluorescence intensity of ethidium, and $\varepsilon_A(\lambda)$ denotes the molar extinction coefficient of TMPyP. $J(\lambda)$ was $1.087 \times 10^{-13} \text{ cm}^3 \text{ mol}^{-1}$ in the absence of Ca^{2+} and $1.108 \times 10^{-13} \text{ cm}^3 \text{ mol}^{-1}$ in the presence of 100 μM Ca^{2+} ion. Given the similar integral values, differences of spectral overlap were not the main factor for enhancement of energy transfer efficiency by Ca^{2+} ions.

Figure 3(b) shows LD^r spectra of DNA and the DNA-TMPyP complex in the presence and absence of 100 μM

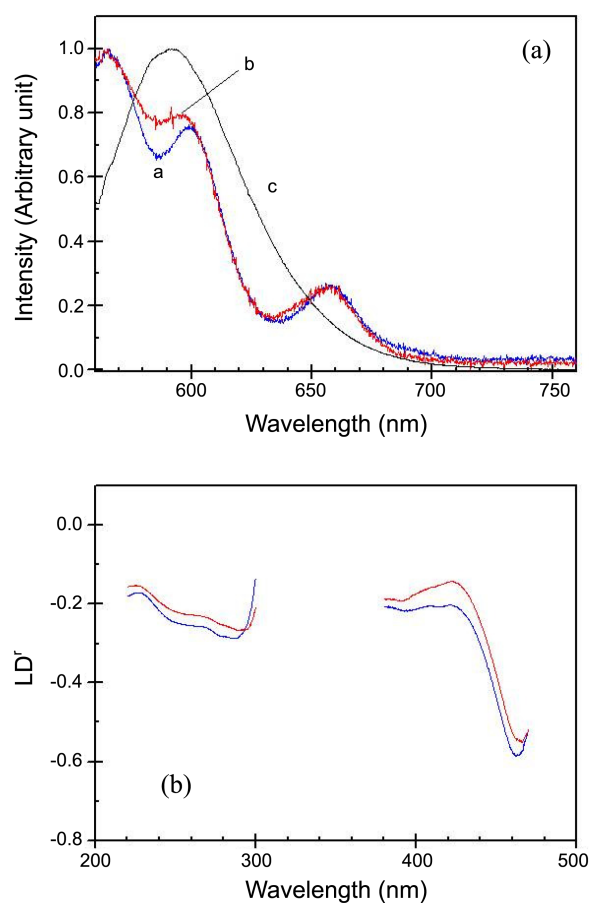


Figure 3. (a) Spectral overlap between the emission spectrum of DNA-bound ethidium (black curve, marked by c) and the absorption spectra of DNA-bound TMPyP in the presence (red, curve b) and absence (blue, curve a) of 100 μM Ca^{2+} . (b) LD^r spectrum obtained from the ratio of the measured LD spectrum and the isotropic absorption spectrum of DNA (black, curve c), and the DNA-TMPyP complex in the presence (red, curve b) and absence (blue, curve a) of 100 μM Ca^{2+} .

Ca^{2+} . The spectra obtained in 20, 40, 60, and 80 μM Ca^{2+} lay between these two spectra and hence are not shown for clarity. The presence of 0.5 μM ethidium did not alter the spectral shape (data not shown). TMPyP intercalates between DNA base pairs²⁹ and as expected for intercalators, the overall magnitude in the Soret region was larger than or comparable to that in the DNA absorption region ($240 \times 280 \text{ nm}$).³⁰ Overall shape of LD^r spectra were similar in the presence and absence of Ca^{2+} : the magnitude slightly decreased in the presence of Ca^{2+} , reflecting increase in the flexibility of DNA as a result of binding of Ca^{2+} to negatively charged phosphate groups of DNA. The large wavelength-dependent LD^r signal in the Soret absorption band suggests differing angles of the B_x and B_y transitions of TMPyP with respect to the DNA helix axis and loss of the degeneracy of these transition moments. This observation suggested that the molecular plane of TMPyP distorted in the intercalation pocket. In this case, the wavelength-dependent LD^r can be analyzed by recognizing that the absorption and LD spectra are the sums of contributions from B_x and B_y transitions.^{14,29}

Both in the presence and the absence of Ca^{2+} , the angle between one of the B_x and the B_y transitions and the local DNA helix axis was near perpendicular ($\sim 86^\circ$), while the other angle was *ca.* 63° . This indicates that the binding geometries of TMPyP and the extent of distortion of the molecular plane of TMPyP in the presence and absence of Ca^{2+} ion were similar in the intercalation pocket.

Discussion

The fluorescence of DNA-intercalated ethidium was quenched by TMPyP which also has been known to intercalate. The quenching efficiency was enhanced by the presence of Ca^{2+} ions. The overlapping of emission spectrum of ethidium and absorption spectrum of TMPyP suggested that the quenching involves, at least in part, the RET mechanism, which originated from electric dipole-dipole interactions between the donor and the acceptor molecules. The concurrent increase in TMPyP's emission intensity also supported the involvement of the RET mechanism. The efficiency of the energy transfer largely depends on the relative orientation between the donor and acceptor molecules, the quantum yield of donor in the absence of acceptor, and the refractive index of the medium. The quantum yield of the ethidium donor could be considered invariant because its emission spectrum was unaltered in the presence of $100 \mu\text{M}$ Ca^{2+} . The change in refractive index by $100 \mu\text{M}$ of Ca^{2+} may be also negligible. Spectral overlap between ethidium's emission and TMPyP's adsorption changed only by about 3%, as it was expected from the similar absorption spectra of TMPyP (Figure 2(a)). This change in spectral overlap was too small to describe large enhancement of energy transfer induced by Ca^{2+} . The orientation factor, κ^2 , can range from 0 to 4,²⁵ depending on the relative orientation of the donor and acceptor molecules. When they are oriented parallel head-to-tail $\kappa^2 = 4$, and when oriented parallel $\kappa^2 = 1$. The variation of κ^2 from 1 to 4 contributes to differences in distance of only 26% because the sixth root of this factor is considered (equation 4). The binding geometry of TMPyP when intercalated in DNA was little affected by the presence of Ca^{2+} , suggesting the retained relative orientation of the donor and the acceptor. Thus, the extent of the change of relative orientation alone may not be enough to account for the doubling of the energy transfer distance by Ca^{2+} . Therefore, neither molecular orientation nor the extent of spectral overlap, nor combination of them was sufficient to elucidate observed effects of Ca^{2+} . Although RET was involved in the observed fluorescence quenching, other factors besides RET must be considered for full elucidation of the enhancement of quenching efficiency by Ca^{2+} .

Quenching of the fluorescence of ethidium intercalated in DNA by various acceptors has been reported to be accompanied by electron transfer. For example, a Rh(III) complex reduced fluorescence intensity by *ca.* 30% at distances of *ca.* 20 \AA ; 10% quenching was observed at *ca.* 30 \AA .³⁰ Divalent transition metal ions bound to DNA have been reported to enhance the electron transfer ability of DNA at

above pH 8.5.³¹⁻³⁴ In such metallic-DNA (M-DNA), transition metal ions, e.g. Zn^{2+} , Co^{2+} , or Ni^{2+} , locate in the middle of the DNA bases, binding to nitrogen in the bases. Alkali and alkali earth metals mainly bind to the phosphate groups of DNA's backbone, with no enhancement of electron transfer activity. In M-DNA, transition metal ions are considered to bind to the bases *via* coordinate covalent bonding, bridging pairs of opposite bases. Thus, the enhancement of electron transfer efficiency is assumed to involve transition metal ions directly participating in the electron transfer mechanism or aiding π - π stacking of the base-pairs. However, alkali earth metal ions bind mainly to the phosphate groups *via* electrostatic interactions and do not exhibit M-DNA behavior. Therefore, an electron transfer mechanism alone may not be sufficient to explain the enhancement of fluorescence quenching by Ca^{2+} . If any electron transfer was involved in observed quenching process, the empty *s* orbital of the Ca^{2+} ions may form partial conducting wires.

Conclusion

Given that neither RET nor electron transfer mechanism could sufficiently explain the observed enhancement of fluorescence quenching by Ca^{2+} , a combination of both mechanisms may be responsible. Detailed DNA-mediated quenching process is under investigation.

Acknowledgments. This research was supported by National Research Foundation of Korea (grant no. 2011-0014336). Dr. J.-M. Kim is thankful for the internal post-doctoral fellowship conferred by Yeungnam University.

References

1. Boon, E. M.; Barton, J. K. *Curr. Opin. Struct. Biol.* **2002**, *12*, 320.
2. Wagenknecht, H.-A. *Nat. Prod. Rep.* **2006**, *23*, 973.
3. Giese, B. *Curr. Opin. Chem. Biol.* **2002**, *6*, 612.
4. Rak, J.; Makowska, J.; Voityuk, A. A. *Chem. Phys.* **2006**, *325*, 567.
5. Sadowska-Aleksiejew, A.; Rak, J.; Voityuk, A. A. *Chem. Phys. Lett.* **2006**, *429*, 546.
6. Kawai, K.; Kodera, H.; Osakada, Y.; Majima, T. *Nature Chem.* **2009**, *1*, 156.
7. Lilley, D. M. J.; Wilson, T. J. *Curr. Opin. Chem. Biol.* **2000**, *4*, 507.
8. Murata, S.-I.; Kucęba, J.; Gryczynski, G. I.; Lakowicz, J. R. *Biopolymers* **2000**, *57*, 306.
9. Kang, J. S.; Lakowicz, J. R. *J. Biochem. Mol. Biol.* **2001**, *34*, 551.
10. Malicka, J.; Gryczynski, I.; Fang, J.; Kusba, J.; Lakowicz, J. R. *Anal. Biochem.* **2003**, *315*, 160.
11. Lee, B. W.; Moon, S. J.; Youn, M. R.; Kim, J. H.; Jang, H. G.; Kim, S. K. *Biophys. J.* **2003**, *85*, 3865.
12. Yun, B. H.; Kim, J.-O.; Lee, B. W.; Lincoln, P.; Nordén, B.; Kim, J.-M.; Kim, S. K. *J. Phys. Chem. B* **2003**, *107*, 9858.
13. Choi, J. Y.; Lee, J.-M.; Lee, H.; Jung, M. J.; Kim, S. K.; Kim, J.-M. *Biophys. Chem.* **2008**, *134*, 56.
14. Jin, B.; Lee, H. M.; Lee, Y.-A.; Ko, J. H.; Kim, C.; Kim, S. K. *J. Am. Chem. Soc.* **2005**, *127*, 2417.
15. Jin, B.; Min, K. S.; Han, S. W.; Kim, S. K. *Biophys. Chem.* **2009**, *144*, 38.
16. Clegg, R. M.; Murchie, A. I.; Zechel, A.; Lilley, D. M. *Proc. Natl. Acad. Sci. U.S.A.* **1993**, *90*, 2994.

17. Deniz, A. A.; Dahan, M.; Grunwell, J. R.; Ha, T.; Faulhaber, A. E.; Chemla, D. S.; Weiss, S.; Schultz, P. G. *Proc. Natl. Acad. Sci. U.S.A.* **1999**, *96*, 3670.
 18. Murphy, M. C.; Rasnik, I.; Cheng, W.; Lohman, T. M.; Ha, T. *Biophys. J.* **2004**, *86*, 2530.
 19. Karymov, M.; Daniel, D.; Sankey, O. F.; Lyubchenko, Y. L. *Proc. Natl. Acad. Sci. U.S.A.* **2005**, *102*, 8186.
 20. Grunwell, J. R.; Glass, J. L.; Lacoste, T. D.; Deniz, A. A.; Chemla, D. S.; Schultz, P. G. *J. Am. Chem. Soc.* **2001**, *123*, 4295.
 21. Heilemann, M.; Tinnefeld, P.; Sanchez Mosteiro, G.; Garcia Parajo, M.; Van Hulst, N. F.; Sauer, M. *J. Am. Chem. Soc.* **2004**, *126*, 6514.
 22. Viasnoff, V.; Meller, A.; Isambert, H. *Nano Letters* **2005**, *6*, 101.
 23. Vyawahare, S.; Eyal, S.; Mathews, K. D.; Quake, S. R. *Nano Letters* **2004**, *4*, 1035.
 24. Pasternack, R. F.; Caccam, M.; Keogh, B.; Stephenson, T. A.; Williams, A. P.; Gibbs, E. J. *J. Am. Chem. Soc.* **1991**, *113*, 6835.
 25. Lakowicz, J. R. *Principles of Fluorescence Spectroscopy*; Springer: New York, 2006.
 26. Jung, J.-A.; Jeon, S. H.; Han, S. W.; Lee, G. J.; Bae, I.-H.; Kim, S. K. *Bull. Korean Chem. Soc.* **2011**, *32*, 2599.
 27. Nordén, B.; Seth, S. *Appl. Spectrosc.* **1985**, *39*, 647.
 28. Nordén, B.; Kubista, M.; Kurucsev, T. Q. *Rev. Biophys.* **1992**, *25*, 51.
 29. Lee, Y.-A.; Lee, S.; Cho, T.-S.; Kim, C.; Han, S. W.; Kim, S. K. *J. Phys. Chem. B* **2002**, *106*, 11351.
 30. Lee, S.; Lee, Y.-A.; Lee, H. M.; Lee, J. Y.; Kim, D. H.; Kim, S. K. *Biophys. J.* **2002**, *83*, 371.
 31. Wettig, S. D.; Li, C. Z.; Long, Y. T.; Kraatz, H. B.; Lee, J. S. *Anal. Sci.* **2003**, *19*, 23.
 32. Rakićin, A.; Aich, P.; Papadopoulos, C.; Kobzar, Y.; Vedenev, A. S.; Lee, J. S.; Xu, J. M. *Phys. Rev. Lett.* **2001**, *86*, 3670.
 33. Aich, P.; Labiuk, S. L.; Tari, L. W.; Delbaere, L. J.; Roesler, W. J.; Falk, K. J.; Steer, R. P.; Lee, J. S. *J. Mol. Biol.* **1999**, *294*, 477.
 34. Aich, P.; Skinner, R. J.; Wettig, S. D.; Steer, R. P.; Lee, J. S. *J. Biomol. Struct. Dyn.* **2002**, *20*, 93.
-